Eur. Phys. J. B **36**, 75–80 (2003)
DOI: 10.1140/epjb/e2003-00318-9

THE EUROPEAN PHYSICAL JOURNAL B

Temperature dependent local Cu-O displacements from underdoped to overdoped La-Sr-Cu-O superconductor

N.L. Saini[1,a], H. Oyanagi[2], T. Ito[2], V. Scagnoli[1], M. Filippi[1], S. Agrestini[1], G. Campi[1], K. Oka[2], and A. Bianconi[1]

[1] Unità INFM, Università di Roma "La Sapienza", P. le Aldo Moro 2, 00185 Roma, Italy
[2] National Institute for Advanced Industrial Science and Technology, 1-1-1 Umezono, Tsukuba, Ibaraki 305-8568, Japan

Received 9 July 2003
Published online 19 November 2003 –

Abstract. We have studied doping evolution of the temperature dependent local Cu-O displacements in the $La_{2-x}Sr_xCuO_4$ superconductor by polarized Cu K-edge extended X-ray absorption fine structure (EXAFS) measurements. While temperature dependent Debye-Waller factor of the Cu-O bonds, measuring the local Cu-O displacements, shows an anomalous increase at low temperature for the underdoped single crystals, we do not find such a dependence for the case of the overdoped system. The results, which are discussed in the light of recent angle resolved photoemission measurements, provide an evidence for some important correlation between the doping dependent electron-lattice interaction, the charge inhomogeneities and the local Cu-O displacements in the copper oxide superconductors.

PACS. 74.72.Dn La-based cuprates – 61.10.Ht X-ray absorption spectroscopy: EXAFS, NEXAFS, XANES, etc. – 74.81.-g Inhomogeneous superconductors and superconducting systems

1 Introduction

Even though character of the superconducting order parameter in the copper oxides with charge 2e remains intact, the electron-lattice interaction, fundamental basis for the superconductivity in metals, is given minor importance in the models for their superconductivity. Further complications are also due to the self-organization of various degrees of freedom, related to the charge, spin and lattice excitations at a mesoscopic length-scale, the phenomena which has been a point of recent debate [1]. However, recent experiments appear to support a key role of local electron-lattice interactions, not only in the superconductivity, but also in the low temperature orders, such as the stripe ordering [2–10].

The main experiments used to probe local displacements in the copper oxides are the pair distribution function (PDF) analysis of neutron and X-ray diffraction, extended X-ray absorption fine structure (EXAFS) and ion channeling [2–7]. Although the techniques have their own limitations to determine quantitative atomic displacements, there is a qualitative agreement on the experimental results obtained by these techniques. Recent technical developments, combining with high brilliance polarized X-ray synchrotron radiation sources, allows the EXAFS spectroscopy, a fast ($\sim 10^{-15}$ s) and local (~5-6 Å) probe [11], to determine the quantitative and directional atomic displacements.

[a] e-mail: saini@romal.infn.it

Here we have exploited the polarized Cu K-edge EXAFS, with high k-resolution, to study the local Cu-O displacements as a function of doping. $La_{2-x}Sr_xCuO_4$ (LSCO) is one of the simplest systems among the copper oxides and hence been chosen as a model system for the present work. The added advantage is that a wide range of hole doping could be achieved by variation of the chemical substitution (Sr content). The temperature dependent distribution of the local and instantaneous lattice distortions (dynamic and static) is measured by the correlated Debye-Waller factor (DWF) of the Cu-O bonds. The DWF shows an anomalous temperature dependence for the underdoped and optimally doped systems, while we do not find such a temperature dependent change for the overdoped case. The anomalous change appears to depend on the electron-lattice interaction, that decreases with increasing the Sr concentration.

2 Experimental

Cu K-edge X-ray absorption measurements were made on a series of $La_{2-x}Sr_xCuO_4$ single crystals ($x = 0.105, 0.13, 0.15, 0.20$) of size $\sim 3\times 2\times 0.5$ mm^3, grown by travelling solvent floating zone (TSFZ) method. The samples show sharp superconducting transitions at the temperatures 28 K, 32 K, 36 K and 29 K respectively with the increasing Sr concentration. The X-ray absorption measurements were performed at the beamline BL13B of the Photon Factory, Tsukuba. The Synchrotron radiation

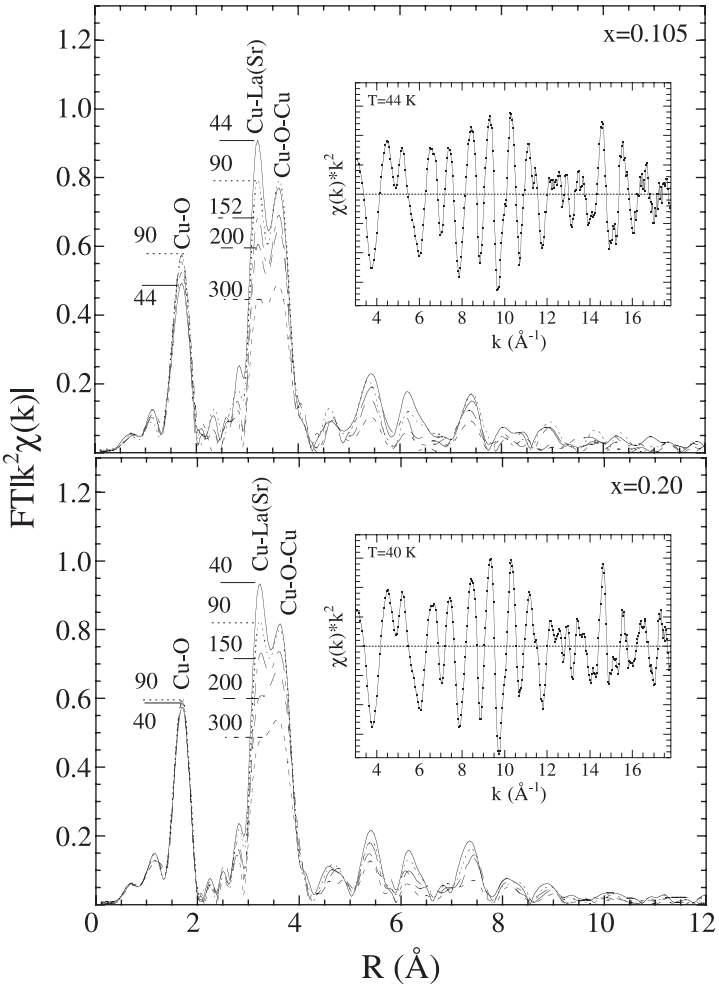

Fig. 1. Fourier transforms of the EXAFS oscillations (multiplied by k^2) of the underdoped $La_{1.895}Sr_{0.105}CuO_4$ (upper) and the overdoped $La_{1.8}Sr_{0.2}CuO_4$ (lower) samples at several temperatures, showing global atomic distribution around the Cu in the two systems. The Fourier transforms are performed for the range k = 3–17 Å^{-1} and not corrected for the phase shifts. The insets show EXAFS oscillations at a representative temperature.

emitted by a 27-pole wiggler source at the 2.5 GeV Photon Factory storage ring was monochromatized by a double crystal Si(111) monochromator and sagittally focused on the samples, mounted in a closed cycle refrigerator. The measurements were made in the grazing incidence geometry with plane polarized light falling parallel to the Cu-O-Cu bonds. This geometry was ascertained by monitoring the $1s \rightarrow 3d_{x^2-y^2}$ quadrupole transition in the absorption spectra [12]. The absorption spectra were recorded by detecting the Cu K_α fluorescence photons using a 19-element Ge X-ray detector array [13]. The sample temperature was controlled and monitored within an accuracy of ±1 K.

X-ray absorption measurements at several temperatures were repeated at the BM29 of the European Synchrotron Radiation Facility (ESRF), Grenoble where the synchrotron radiation emitted by a Bending magnet was monochromatized by a double crystal Si(311) monochromator. As our standard experimental approach, several absorption scans were collected to limit the noise level to the order of 10^{-4}. Standard procedure was used to extract the EXAFS signal from the absorption spectrum [11], followed by the correction of the signal for the X-ray fluorescence self-absorption effects [14] before the analysis. Further details on the experiments and the data analysis could be found in our earlier publications [6,7,12].

3 Results and discussion

Figure 1 shows the Fourier transforms of the EXAFS oscillations (weighted by k^2) measured on the underdoped ($La_{1.895}Sr_{0.105}CuO_4$) and the overdoped ($La_{1.8}Sr_{0.2}CuO_4$) samples at several temperatures. The EXAFS oscillations (weighted by k^2) at representative temperatures are shown as inset. The Fourier transforms (FTs) were performed between k_{min} = 3 Å^{-1} and k_{max} = 17 Å^{-1} using a Gaussian window. The FTs are not corrected by the phase shifts due to photoelectron back-scattering and represent the raw experimental data. The first peak in the Fourier transform corresponds to the in-plane Cu-O bonds, while the doublet structure at ∼3–4 Å is due to the Cu-La(Sr) and

the Cu-O-Cu multiple scattering signals. The doublet appears more pronounced and the first peak due to the Cu-O scattering shows stronger temperature dependence for the underdoped system.

Looking at the temperature dependence we can see a clear increase of the the Cu-La(Sr) and Cu-O-Cu peaks with decreasing temperature, however, the Cu-O peak does not show this usual temperature dependence. Indeed, while Cu-O peak for the underdoped system shows an anomalous change (e.g., amplitude of the Cu-O peak at 44 K is lower than the one at 300 K), there is hardly any temperature dependence of this peak for the overdoped sample. Here we focus on the atomic displacements in the electronically active CuO_2 plane (i.e. the in-plane Cu-O bond) and their evolution with the doping. The EXAFS signal due to the Cu-O bonds is well separated from the longer bond contributions and hence can be easily analyzed separately. We have used the standard procedure for the analysis of the EXAFS data considering a single Cu-O bond distance for the coordination shell, where the effective Debye Waller factor (DWF) includes the main distortion effects. This approach is adopted to make a direct comparison of the temperature dependent Cu-O displacements with doping. Quantitative value of the DWF (σ^2) depends on the technical aspects (the experimental geometry and the analysis). Although, this is irrelevant for the temperature dependence, we have made all efforts to determine quantitative values of the σ^2 (within the reported uncertainties) by performing the measurements in the same experimental conditions and applying the same data analysis procedure for all the crystals, simulated in the same k ($k = 3{-}17$ Å^{-1}) range.

The number of parameters which may be determined by EXAFS is limited by the number of independent data points: $N_{ind} \sim (2\Delta k \Delta R)/\pi$, where Δk and ΔR are respectively the ranges in the k and the R space over which the data are analyzed [11]. In the present case $\Delta k = 14$ Å^{-1} and $\Delta R = 1$ Å give $N_{ind} \sim 9$ for the first shell EXAFS. Except the radial distance R and the DWF σ^2, all the other parameters were kept constant (the S_0^2, amplitude correction factor due to photoelectron correlation, also called passive electrons reduction factor was fixed to 0.68 while the photoelectron energy origin, E_0, was fixed to -2.4 eV with respect to the Cu K-edge absorption jump) in the conventional least squares paradigm following the standard approach and our experience on the similar systems [6,7,12]. Starting parameters were taken from the diffraction studies [15]. Figure 2 shows representative fits for the isolated Cu-O EXAFS. With a reasonably good fits at the higher k-values, we think that the derived parameters (the radial distance R and the σ^2) represent the actual behavior. Although the quantitative value of the DWF depends on the structural models used [6], it is irrelevant for the temperature dependent behavior, reported in this work. The approach to fit with a Gaussian distribution was assumed (commonly used in EXAFS) to make a direct comparison of the temperature and the doping dependent displacements. The uncertainties in the derived parameters were estimated by the standard EXAFS method in

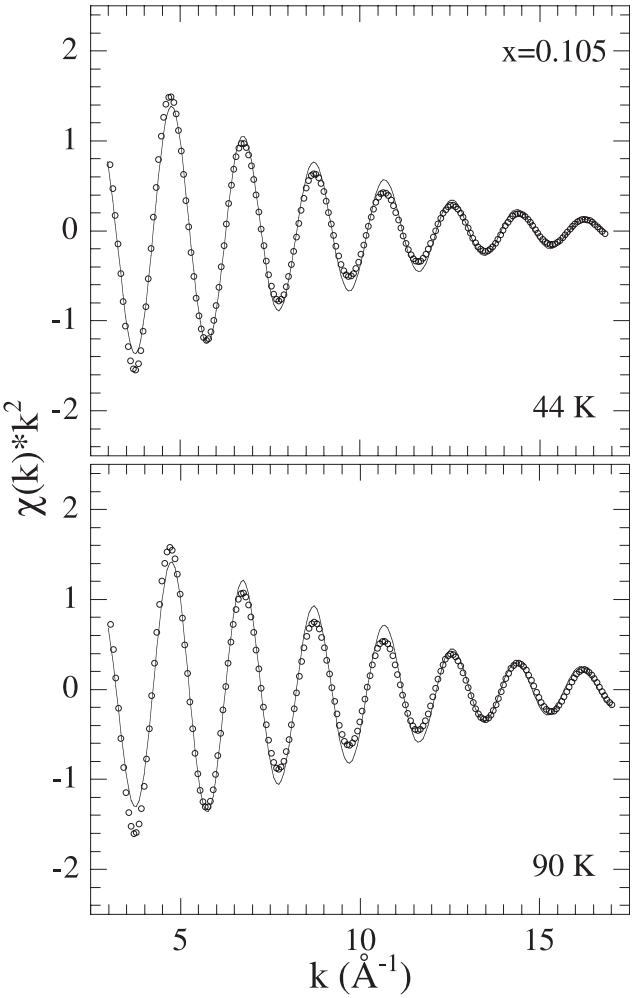

Fig. 2. Representative fits (solid line) to the isolated Cu-O EXAFS (multiplied by k^2) for the $La_{1.895}Sr_{0.105}CuO_4$ system at 44 K (upper) and 90 K (lower).

which the quality of the fit parameter, proportional to the statistical χ^2, is determined as a function of the concerned parameter (R and the σ^2) for the uncertainty estimation. The uncertainties are usually estimated from a fractional increase of the χ^2 above its minimum value. This fraction, which depends on several experimental and data analysis factors, was established by analyzing four independent EXAFS scans at each temperature. The average distances were found to be independent of the temperature within the experimental uncertainties and are similar to the one determined by the diffraction experiments.

The temperature dependence of the Cu-O DWF is shown in Figure 3 with the variable Sr content. From the temperature dependence of the σ^2, we can see some evident differences between the underdoped and the overdoped samples. While the underdoped and the optimally doped systems show anomalous temperature dependence, we do not see any evident temperature dependent anomaly for the overdoped case. The temperature dependences of the σ^2 are anomalous, with an increase at a temperature T_s, followed by the small decrease at

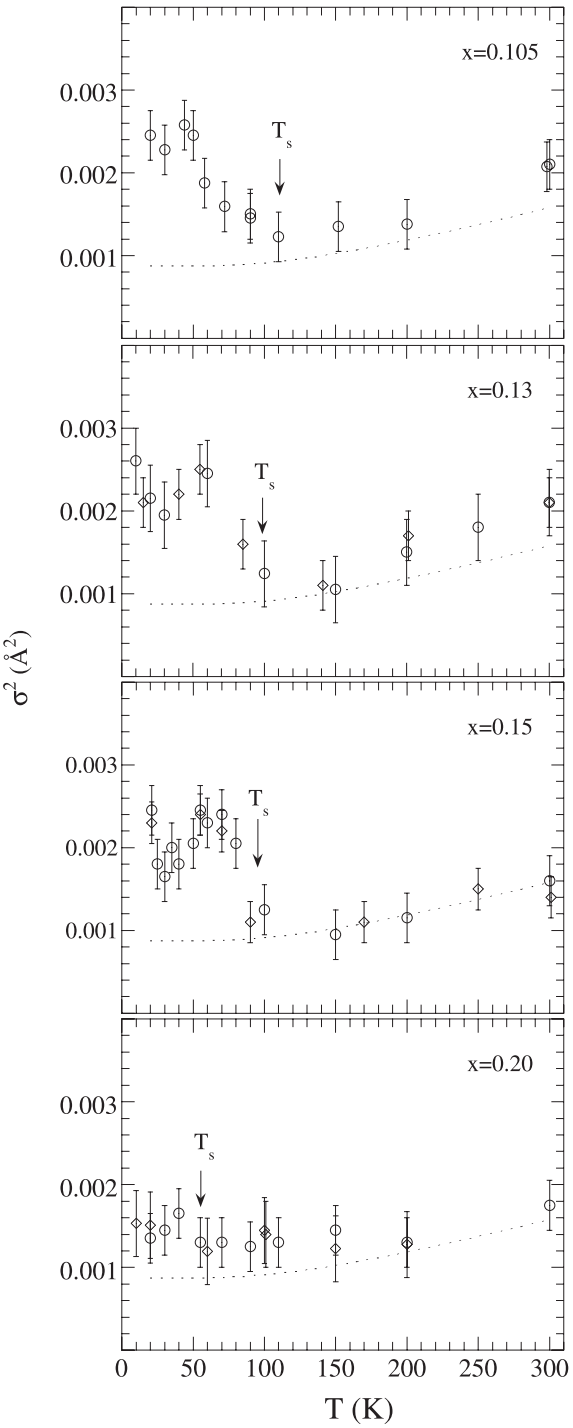

Fig. 3. Temperature dependence of the correlated Debye-Waller factors (symbols) of the Cu-O pairs (σ^2) for the underdoped $La_{1.895}Sr_{0.105}CuO_4$ (upper) and $La_{1.87}Sr_{0.13}CuO_4$ (upper middle), the optimally doped $La_{1.85}Sr_{0.15}CuO_4$ (lower middle) and the overdoped $La_{1.8}Sr_{0.2}CuO_4$ (lower) samples. The expected temperature dependence of the Debye-Waller factor for a fully correlated motion of Cu and O is shown by the dotted lines. Different symbols in the plots correspond to different data sets. The underdoped and the optimally doped samples reveal a clear upturn (with a variable amplitude) in the DWF around 100 K, while the upturn is less evident in the overdoped case it seems to appear at a lower temperature. Approximate values of T_s are indicated.

the superconducting transition temperature T_c. The increase in the σ^2 at T_s is evident for the underdoped ($La_{1.895}Sr_{0.105}CuO_4$ and $La_{1.87}Sr_{0.13}CuO_4$) and optimally doped ($La_{1.85}Sr_{0.15}CuO_4$) system, however, the overdoped ($La_{1.8}Sr_{0.2}CuO_4$) system shows a negligible change. On the other hand, the drop in the σ^2 at the T_c is better seen only for the slightly underdoped and the optimally doped systems.

It is known that at the appearance of any charge density wave like instability the DWF shows an anomalous change as found in several density wave systems [16]. Indeed the σ^2 shows an anomalous upturn at T_s, that appears to be due to such an instability (driven by a particular local lattice distortion in the CuO_2 plane [6,7]). It is worth recalling that a model system $La_{1.48}Sr_{0.12}Nd_{0.4}CuO_4$ [17–20], showing stripe order, reveals similar temperature dependent σ^2 [21]. Considering these experimental facts, we think that the anomalous upturn in the σ^2 (Fig. 3) could be due to a charge instability related to the charge stripe ordering. Sharma et al. [3] have found a similar change in the temperature dependence of the excess displacements (a parameter analogous to the DWF measuring dynamic and static distortions) measured by the ion-channeling on the $YBa_2Cu_3O_{6+\delta}$ superconducting system at the stripe ordering temperature. Below the T_s the pair distribution function for the Cu-O exhibits a width larger than that expected to be due to thermal fluctuations with an asymmetric bond length distribution [6,7].

Within the experimental temperature points, it is hard to claim any change in the temperature T_s, however, there seems a decrease in the amplitude of the σ^2 upturn with increasing the doping. Figure 4 shows the estimated amplitude of the upturn at the T_s as a function Sr content. Even though the change in the upturn with doping is small, it appears to indicate some relation with the doping dependent charge inhomogeneity in the copper oxides. It was shown earlier that the upturn at T_s is due to asymmetric pair distribution function derived by splitting of the Cu-O bonds [6,7]. Therefore the amplitude appears to provide a measure of the barrier height in the multi-well potential. The present data seems to indicate decrease of the barrier height with the increasing doping.

Here we attempt to understand the results in the light of the angle resolved photoemission spectroscopy (ARPES) data revealing a kink in the band dispersion, defined by an abrupt change of the electron velocity at ∼50–80 meV [8]. This kink has been interpreted to be due to the phonons associated with the movement of the oxygen atoms related to the electron-lattice coupling. In Figure 4 we have also plotted doping dependence of the electron-lattice coupling, estimated from the ARPES data on the $La_{2-x}Sr_xCuO_4$ using the two velocities, i.e., dressed velocity and the bare velocity of the electrons. The electron-lattice coupling shows a continuous decrease with the doping. This behavior of the electron-lattice interaction, analogous to the σ^2 upturn amplitude appears to suggest that the kink structure could be related to the Cu-O displacements, with asymmetric bond

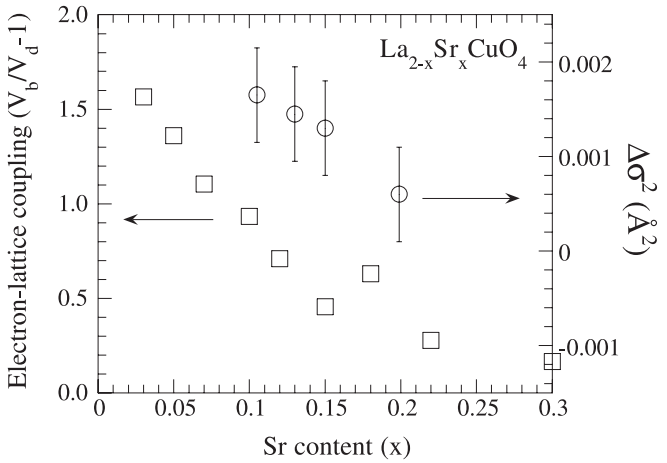

Fig. 4. Amplitude of the upturn of the temperature dependent DWF (Fig. 3) as a function of doping (open circles), showing a decreasing trend with the increasing doping. The upturn has been estimated from the Figure 3, as the maximum change in the DWF across the T_s. The electron lattice coupling estimated from the ARPES data on the $La_{2-x}Sr_xCuO_4$ system [8] as a function of doping, revealing a kink structure in the dispersion is also shown (open squares). The electron lattice coupling is determined using the bare (V_b) and the dressed (V_d) electron velocities.

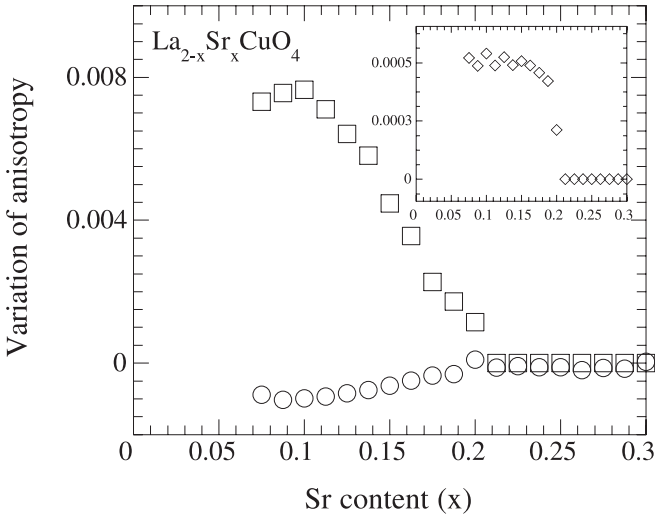

Fig. 5. Doping dependence of the change in the in-plane (open squares) and out-of-plane (open circles) structural anisotropy while the sample is cooled from room temperature (295 K) to the low temperature (10 K), estimated using the published neutron diffraction data [15]. The in-plane anisotropy is determined by the ratio of crystallographic a and b-axes, while the out-of plane anisotropy is given by ratio of average in-plane lattice parameter and the c-axis. The plot represents difference of the in-plane and out of plane anisotropy at two temperatures. Change in the in-plane anisotropy from 70 K and 10 K is shown as an inset. The plot represents the difference in the anisotropy at the two measured temperatures.

distribution, driving the system in an inhomogeneous charge state with self-organization in stripes. Thus the negligibly small anomaly in the temperature dependent displacements for the overdoped system seems to be due to reduced electron-lattice interaction and increased kinetic energy of the electron in the homogeneous state.

Let us compare the doping dependent local structure measured by the EXAFS with the diffraction studies. Considering several experimental evidences we assume that the system goes into an inhomogeneous state with the in-plane charge stripe ordering at low temperature [1,2,4–7,9,10,17–25]. In the EXAFS results this has been revealed by an upturn in the correlated DWF measuring the instantaneous displacements in the CuO_2 plane. The stripe ordering in the CuO_2 plane is expected to introduce an in-plane anisotropy, however, this anisotropy could be easily washed out due to the twinning of the orthorhombic unit cell and hence generally ignored in the diffraction studies. Here we have given a careful look to the diffraction data and the estimated doping dependent in-plane and out of plane structural anisotropy in the LSCO system at different temperatures.

Figure 5 shows the doping dependence of the change in the in-plane and out-of-plane structural anisotropy while the sample is cooled from room temperature (295 K) to the low temperature (10 K), estimated using the published neutron diffraction data [15]. Doping dependent change in the in-plane anisotropy from 70 K to 10 K is shown as an inset. While the temperature dependent change in the in-plane structural anisotropy shows a clear decrease with the increasing doping, the out-of-plane anisotropy reveals a comparatively small change. In other words, the hole doping in the CuO_2 plane, introduced by the Sr substitution, seems to make the system more rigid and hence the temperature dependent change in the in-plane structural anisotropy decreases continuously with the increasing doping. While the system is overdoped, the structural anisotropy (in-plane/out-of-plane) shows a negligible change with the temperature. The results are analogous to the decrease of the temperature dependent upturn in the DWF with the increasing doping. The observation is also consistent with the fact that the host lattice in the underdoping range is more susceptible to the external conditions (impurities, pressure, magnetic field, temperature etc.). For example impurities strongly suppress the superconducting transition temperature in the underdoped systems while the effect is small on the overdoped case [26]. In addition, it is known that the T_c increases under external pressure [27] and strain modulation [28] in the underdoped range, while the change is very small for the overdoped case. This indicates that a particular electron-lattice interaction, decreasing with increasing doping, seems a key parameter for the characteristic properties of the copper oxide superconductors.

In summary, we have measured temperature and doping dependent local Cu-O displacements in the LSCO superconductor by high resolution polarized Cu K-edge EXAFS. The correlated DWF has been taken as an order parameter of the instantaneous Cu-O displacements. We find that the local Cu-O displacements show anomalous change at a temperature T_s, with variable amplitude as a function of doping. The amplitude of the upturn decreases

with the increasing doping. We have attempted to understand the results in terms of the doping induced change in the electron-lattice interaction, that decreases with the increasing doping, as seen by a kink structure in the angle resolved photoemission experiments. The findings, showing a local structural crossover from the underdoping to the overdoping, suggest that a particular distortion of the CuO_2 plane should be involved in the electron-lattice interaction leading to the kink structure in the band dispersion near the Fermi level, as shown by the ARPES data. Considering the existing facts, we can conclude that the increasing electron-lattice interaction drives the Cu-O potential to a multiwell like at low temperature, which gets single well like at the small electron-lattice interaction. Nevertheless, the results presented here have direct implication on the correlating electron-lattice interaction, the inhomogeneous state and the high T_c superconductivity in the complex copper oxides.

The authors thank the PF and ESRF staff for their cooperation during the experiments. This research has been supported by the MURST (under the project cofinanziamento Leghe e composti intermetallici: stabilità termodinamica, proprietà fisiche e reattività), by the INFM (under the project PA-LLDS-SCS), and by the CNR (under the project 5% Superconduttività).

References

1. *Stripes and Related Phenomena,* edited by A. Bianconi, N.L. Saini (Kluwer Academics/Plenum Publishers, New York, 2000); also see e.g. the speciale issues of J. Supercond. **10**, No. 4 (1997) and Int. J. Mod. Phys. B **14**, No. 29-31 (2000)
2. A. Lanzara, G.-M. Zhao, N.L. Saini, A. Bianconi, K. Conder, H. Keller, K.A. Müller, J. Phys.: Condens. Matter **11**, L541 (1999)
3. R.P. Sharma, S.B. Ogale, Z.H. Zhang, J.R. Liu, W.K. Wu, B. Veal, A. Paulikas, H. Zhang, T. Venkatesan, Nature **404**, 736 (2000), and references therein; R.P. Sharma et al., unpublished (2002)
4. E.S. Bozin, G.H. Kwei, H. Takagi, S.J.L. Billinge, Phys. Rev. Lett. **84**, (2000) 5856, and references therein
5. R.J. McQueeney, Y. Petrov, T. Egami, M. Yethiraj, G. Shirane, Y. Endoh, Phys. Rev. Lett. **82**, 628 (1999)
6. N.L. Saini, A. Bianconi, H. Oyanagi, J. Phys. Soc. Jpn **70**, 2092 (2001)
7. A. Bianconi, N.L. Saini, A. Lanzara, M. Missori, T. Rossetti, H. Oyanagi, H. Yamaguchi, K. Oka, T. Ito, Phys. Rev. Lett. **76**, (1996) 3412; N.L. Saini, A. Lanzara, H. Oyanagi, H. Yamaguchi, K. Oka, T. Ito, A. Bianconi, Phys. Rev. B **55**, (1997) 12759; N.L. Saini, A. Lanzara, A. Bianconi, H. Oyanagi, H. Yamaguchi. K. Oka, T. Ito, Physica C **268**, 121 (1996)
8. A. Lanzara, P.V. Bogdanov, X.J. Zhou, S.A. Kellar, D.L. Feng, E.D. Lu, T. Yoshida, H. Eisaki, A. Fujimori, K. Kishio, J.-I. Shimoyama, T. Noda, S. Uchida, Z. Hussain, Z.-X. Shen, Nature **412**, 510 (2001)
9. J.-S. Zhou, J.B. Goodenough, Phys. Rev. B **56**, 6288 (1997); J.B. Goodenough, J.S. Zhou, Nature **386**, 229 (1997)
10. K.A. Müller, in *Stripes and Related Phenomena*, edited by A. Bianconi, N.L. Saini (Kluwer Academic/Plenum Publishers, New York, 2000), p. 1
11. *X-Ray Absorption: Principle, Applications Techniques of EXAFS, SEXAFS and XANES*, edited by R. Prinz, D. Koningsberger (J. Wiley and Sons, New York, 1988)
12. N.L. Saini, A. Lanzara, A. Bianconi, H. Oyanagi, Phys. Rev. B **58**, 11768 (1998)
13. H. Oyanagi, R. Shioda, Y. Kuwahara, K. Haga, J. Synchrotron Rad. **2**, (1995) 99; ibid. **5**, 48 (1998)
14. L. Tröger, D. Arvanitis, K. Baberschke, H. Michaelis, U. Grimm, E. Zschech, Phys. Rev. B **46**, 3283 (1992); J. Goulon, C. Goulon-Ginet, R. Cortes, J.M. Dubois, J. Phys. I France **43**, 539 (1982)
15. P.G. Radaelli, D.G. Hinks, W. Mitchell, B.A. Hunter, J.L. Wagner, B. Dabrowski, K.G. Vandervoort, H.K. Viswanathan, J.D. Jorgensen, Phys. Rev. B **49**, 4163 (1992)
16. G. Grüner, *Density Waves in Solids*, Frontiers in Physics Vol. 89 (Addison-Wesley, USA, 1994)
17. N. Ichikawa, S. Uchida, J.M. Tranquada, T. Niemöller, P.M. Gehring, S.-H. Lee, J.R. Schneider, Phys. Rev. Lett. **85**, 1738 (2000) and references therin
18. X.J. Zhou, P. Bogdanov, S.A. Kellar, T. Noda, H. Eisaki, S. Uchida, Z. Hussain, Z.-X. Shen, Science **286**, 268 (1999)
19. T. Noda, H. Eisaki, S. Uchida, Science **286**, 265 (1999)
20. S. Tajima, T. Noda, H. Eisaki, S. Uchida, Phys. Rev. Lett. **86**, 500 (2001)
21. N.L. Saini, H. Oyanagi A. Lanzara, D. Di Castro, S. Agrestini, A. Bianconi, F. Nakamura, T. Fujita, Phys. Rev. B **64**, 132510 (2001)
22. K.A. Müller, G.-M. Zhao, K. Conder, H. Keller, J. Phys.: Condens. Matter **10**, L291 (1998)
23. A.W. Hunt, P.M. Singer, K.R. Thruber, T. Imai, Phys. Rev. Lett. **82**, 4300 (1999); P.M. Singer, A.W. Hunt, A.F. Cederström, T. Imai, Phys. Rev. B **60**, 15345 (1999)
24. K. Yamada, C.H. Lee, K. Kurahashi, J. Wada, S. Wakimoto, S. Ueki, H. Kimura, Y. Endoh, S. Hosoya, G. Shirane, R.J. Birgeneau, M. Greven, M.A. Kastner, Y.J. Kim, Phys. Rev. B **57**, 6165 (1998)
25. P.C. Hammel, B.W. Statt, R.L. Martin, F.C. Chou, D.C. Johnston, S.-W. Cheong, Phys. Rev. B **57**, R712, (1998); B.W. Statt, P.C. Hammel, Z. Fisk, S.-W. Cheong, F.C. Chou, D.C. Johnston, J.E. Schirber, Phys. Rev. B **52**, 15575 (1995)
26. J.L. Tallon, C. Bernhard, G.V.M. Williams, J.W. Loram, Phys. Rev. Lett. **79**, 5294 (1997); T. Kluge, Y. Koike, A. Fujiwara, M. Kato, T. Noji, Y. Saito, Phys. Rev. B **52**, R727 (1995)
27. J.S. Schilling, J. Phys. Chem. Solids **59**, 553 (1998)
28. H. Sato, A. Tsukada, M. Naito, A. Matsuda, Phys. Rev. B **61**, 12447 (2000); J.P. Locquet, J. Perret, J. Fompeyrine, E. Mchler, J.W. Seo, G. Van Tendelloo, Nature **394**, 453 (1998); J.P Attfield, A.L Kharlanov, J.A. McAllister, Nature **394**, 157 (1998); I. Bozovic, G. Logvenov, I. Belca, B. Narimbetov, I. Sveklo, Phys. Rev. Lett. **89**, 107001 (2002)